
Federated Model Heterogeneous Matryoshka Representation Learning

Liping Yi^{1,2}, Han Yu², Chao Ren², Gang Wang¹, Xiaoguang Liu¹, Xiaoxiao Li³

¹College of Computer Science, TMCC, SysNet, DISSec, GTIISC, Nankai University

²College of Computing and Data Science, Nanyang Technological University

³Department of Electrical and Computer Engineering, The University of British Columbia

yiliping@nbj1.nankai.edu.cn

Abstract

Model heterogeneous federated learning (MHeteroFL) enables FL clients to collaboratively train models with heterogeneous structures in a distributed fashion. However, existing MHeteroFL methods rely on training loss to transfer knowledge between the client model and the server model, resulting in limited knowledge exchange. To address this limitation, we propose the Federated model heterogeneous Matryoshka Representation Learning (FedMRL) approach for supervised learning tasks. It adds an auxiliary small homogeneous model shared by clients with heterogeneous local models. (1) The generalized and personalized representations extracted by the two models' feature extractors are fused by a personalized lightweight representation projector. This step enables representation fusion to adapt to local data distribution. (2) The fused representation is then used to construct Matryoshka representations with multi-dimensional and multi-granular embedded representations learned by the global homogeneous model header and the local heterogeneous model header. This step facilitates multi-perspective representation learning and improves model learning capability. Theoretical analysis shows that FedMRL achieves a $\mathcal{O}(1/T)$ non-convex convergence rate. Extensive experiments on benchmark datasets demonstrate its superior model accuracy with low communication and computational costs compared to seven state-of-the-art baselines. It achieves up to 8.48% and 24.94% accuracy improvement compared with the state-of-the-art and the best same-category baseline, respectively.

1 Introduction

Traditional federated learning (FL) [29] often relies on a central FL server to coordinate multiple data owners (a.k.a., FL clients) to train a global shared model without exposing local data. In each communication round, the server broadcasts the global model to the clients. A client trains it on its local data and sends the updated local model to the FL server. The server aggregates local models to produce a new global model. These steps are repeated until the global model converges.

However, the above design cannot handle the following heterogeneity challenges [49] commonly found in practical FL applications: (1) Data heterogeneity [40, 45, 44, 47, 39, 55]: FL clients' local data often follow non-independent and identically distributions (non-IID). A single global model produced by aggregating local models trained on non-IID data might not perform well on all clients. (2) System heterogeneity [11, 46, 48]: FL clients can have diverse system configurations in terms of computing power and network bandwidth. Training the same model structure among such clients means that the global model size must accommodate the weakest device, leading to sub-optimal performance on other more powerful clients. (3) Model heterogeneity [41]: When FL clients are

enterprises, they might have heterogeneous proprietary models which cannot be directly shared with others during FL training due to intellectual property (IP) protection concerns.

To address these challenges, the field of model heterogeneous federated learning (MHeteroFL) [52, 49, 53, 54, 51, 50] has emerged. It enables FL clients to train local models with tailored structures suitable for local system resources and local data distributions. Existing MHeteroFL methods [38, 43] are limited in terms of knowledge transfer capabilities as they commonly leverage the training loss between server and client models for this purpose. This design leads to model performance bottlenecks, incurs high communication and computation costs, and risks exposing private local model structures and data.

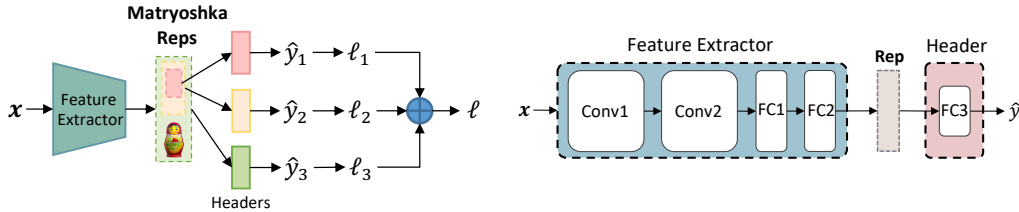


Figure 1: Left: Matryoshka Representation Learning. Right: Feature extractor and prediction header.

Recently, Matryoshka Representation Learning (MRL) [21] has emerged to tailor representation dimensions based on the computational and storage costs required by downstream tasks to achieve a near-optimal trade-off between model performance and inference costs. As shown in Figure 1(left), the representation extracted by the feature extractor is constructed to form Matryoshka Representations involving a series of embedded representations ranging from low-to-high dimensions and coarse-to-fine granularities. Each of them is processed by a single output layer for calculating loss, and the sum of losses from all branches is used to update model parameters. This design is inspired by the insight that people often first perceive the coarse aspect of a target before observing the details, with multi-perspective observations enhancing understanding.

Inspired by MRL, we address the aforementioned limitations of MHeteroFL by proposing the Federated model heterogeneous Matryoshka Representation Learning (FedMRL) approach for supervised learning tasks. For each client, a shared global auxiliary homogeneous small model is added to interact with its heterogeneous local model. Both two models consist of a feature extractor and a prediction header, as depicted in Figure 1(right). FedMRL has two key design innovations. **(1) Adaptive Representation Fusion:** for each local data sample, the feature extractors of the two local models extract generalized and personalized representations, respectively. The two representations are spliced and then mapped to a fused representation by a lightweight personalized representation projector adapting to local non-IID data. **(2) Multi-Granularity Representation Learning:** the fused representation is used to construct Matryoshka Representations involving multi-dimension and multi-granularity embedded representations, which are processed by the prediction headers of the two models, respectively. The sum of their losses is used to update all models, which enhances the model learning capability owing to multi-perspective representation learning.

The personalized multi-granularity MRL enhances representation knowledge interaction between the homogeneous global model and the heterogeneous client local model. Each client’s local model and data are not exposed during training for privacy-preservation. The server and clients only transmit the small homogeneous models, thereby incurring low communication costs. Each client only trains a small homogeneous model and a lightweight representation projector in addition, incurring low extra computational costs. We theoretically derive the $\mathcal{O}(1/T)$ non-convex convergence rate of FedMRL and verify that it can converge over time. Experiments on benchmark datasets comparing FedMRL against seven state-of-the-art baselines demonstrate its superiority. It improves model accuracy by up to 8.48% and 24.94% over the best baseline and the best same-category baseline, while incurring lower communication and computation costs.

2 Related Work

Existing MHeteroFL works can be divided into the following four categories.

MHeteroFL with Adaptive Subnets. These methods [3–5, 11, 14, 56, 64] construct heterogeneous local subnets of the global model by parameter pruning or special designs to match with each client’s

local system resources. The server aggregates heterogeneous local subnets wise parameters to generate a new global model. In cases where clients hold black-box local models with heterogeneous structures not derived from a common global model, the server is unable to aggregate them.

MHeteroFL with Knowledge Distillation. These methods [6, 8, 9, 15–17, 22, 23, 25, 27, 30, 32, 35, 36, 42, 57, 59] often perform knowledge distillation on heterogeneous client models by leveraging a public dataset with the same data distribution as the learning task. In practice, such a suitable public dataset can be hard to find. Others [12, 60, 61, 63] train a generator to synthesize a shared dataset to deal with this issue. However, this incurs high training costs. The rest (FD [19], FedProto [41] and others [1, 2, 13, 49, 58]) share the intermediate information of client local data for knowledge fusion.

MHeteroFL with Model Split. These methods split models into feature extractors and predictors. Some [7, 10, 31, 33] share homogeneous feature extractors across clients and personalize predictors, while others (LG-FedAvg [24] and [18, 26]) do the opposite. Such methods expose part of the local model structures, which might not be acceptable if the models are proprietary IPs of the clients.

MHeteroFL with Mutual Learning. These methods (FedAPEN [34], FML [38], FedKD [43] and others [28]) add a shared global homogeneous small model on top of each client’s heterogeneous local model. For each local data sample, the distance of the outputs from these two models is used as the mutual loss to update model parameters. Nevertheless, the mutual loss only transfers limited knowledge between the two models, resulting in model performance bottlenecks.

The proposed FedMRL approach further optimizes mutual learning-based MHeteroFL by enhancing the knowledge transfer between the server and client models. It achieves personalized adaptive representation fusion and multi-perspective representation learning, thereby facilitating more knowledge interaction across the two models and improving model performance.

3 The Proposed FedMRL Approach

FedMRL aims to tackle data, system, and model heterogeneity in supervised learning tasks, where a central FL server coordinates N FL clients to train heterogeneous local models. The server maintains a global homogeneous small model $\mathcal{G}(\theta)$ shared by all clients. Figure 2 depicts its workflow ¹:

- ① In each communication round, K clients participate in FL (*i.e.*, the client participant rate $C = K/N$). The global homogeneous small model $\mathcal{G}(\theta)$ is broadcast to them.
- ② Each client k holds a heterogeneous local model $\mathcal{F}_k(\omega_k)$ ($\mathcal{F}_k(\cdot)$ is the heterogeneous model structure, and ω_k are personalized model parameters). Client k simultaneously trains the heterogeneous local model and the global homogeneous small model on local non-IID data D_k (D_k follows the non-IID distribution P_k) via personalized Matryoshka Representations Learning with a personalized representation projector $\mathcal{P}_k(\varphi_k)$.
- ③ The updated homogeneous small models are uploaded to the server for aggregation to produce a new global model for knowledge fusion across heterogeneous clients.

The objective of FedMRL is to minimize the sum of the loss from the combined models ($\mathcal{W}_k(w_k) = (\mathcal{G}(\theta) \circ \mathcal{F}_k(\omega_k) | \mathcal{P}_k(\varphi_k))$) on all clients, *i.e.*,

$$\min_{\theta, \omega_0, \dots, \omega_{N-1}} \sum_{k=0}^{N-1} \ell(\mathcal{W}_k(D_k; (\theta \circ \omega_k | \varphi_k))). \quad (1)$$

These steps repeat until each client’s model converges. After FL training, a client uses its local combined model without the global header for inference. ²

3.1 Adaptive Representation Fusion

We denote client k ’s heterogeneous local model feature extractor as $\mathcal{F}_k^{ex}(\omega_k^{ex})$, and prediction header as $\mathcal{F}_k^{hd}(\omega_k^{hd})$. We denote the homogeneous global model feature extractor as $\mathcal{G}^{ex}(\theta^{ex})$ and prediction header as $\mathcal{G}^{hd}(\theta^{hd})$. Client k ’s local personalized representation projector is denoted as $\mathcal{P}_k(\varphi_k)$. In

¹Algorithm 1 in Appendix A describes the FedMRL algorithm.

²Appendix C.3 provides experimental evidence for inference model selection.

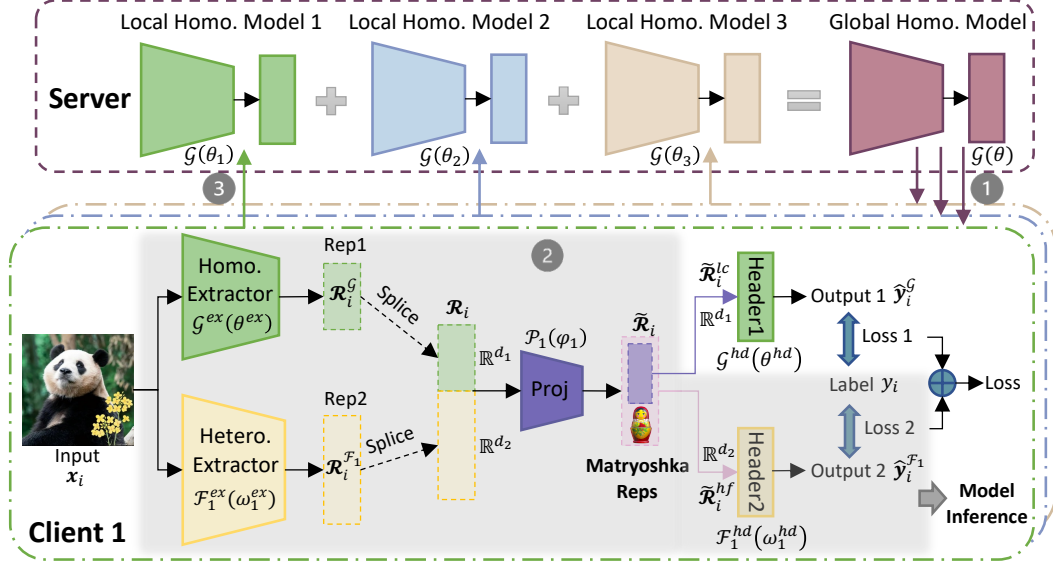


Figure 2: The workflow of FedMRL.

the t -th communication round, client k inputs its local data sample $(x_i, y_i) \in D_k$ into the two feature extractors to extract generalized and personalized representations as:

$$\mathcal{R}_i^G = \mathcal{G}^{ex}(x_i; \theta^{ex, t-1}), \mathcal{R}_i^{F_k} = \mathcal{F}_k^{ex}(x_i; \omega_k^{ex, t-1}). \quad (2)$$

The two extracted representations $\mathcal{R}_i^G \in \mathbb{R}^{d_1}$ and $\mathcal{R}_i^{F_k} \in \mathbb{R}^{d_2}$ are spliced as:

$$\mathcal{R}_i = \mathcal{R}_i^G \circ \mathcal{R}_i^{F_k}. \quad (3)$$

Then, the spliced representation is mapped into a fused representation by the lightweight representation projector $\mathcal{P}_k(\varphi_k^{t-1})$ as:

$$\tilde{\mathcal{R}}_i = \mathcal{P}_k(\mathcal{R}_i; \varphi_k^{t-1}), \quad (4)$$

where the projector can be a one-layer linear model or multi-layer perceptron. The fused representation $\tilde{\mathcal{R}}_i$ contains both generalized and personalized feature information. It has the same dimension as the client's local heterogeneous model representation \mathbb{R}^{d_2} , which ensures the representation dimension \mathbb{R}^{d_2} and the client local heterogeneous model header parameter dimension $\mathbb{R}^{d_2 \times L}$ (L is the label dimension) match.

The representation projector can be updated as the two models are being trained on local non-IID data. Hence, it achieves personalized representation fusion adaptive to local data distributions. Splicing the representations extracted by two feature extractors can keep the relative semantic space positions of the generalized and personalized representations, benefiting the construction of multi-granularity Matryoshka Representations. Owing to representation splicing, the representation dimensions of the two feature extractors can be different (*i.e.*, $d_1 \leq d_2$). Therefore, we can vary the representation dimension of the small homogeneous global model to improve the trade-off among model performance, storage requirement and communication costs.

In addition, each client's local model is treated as a black box by the FL server. When the server broadcasts the global homogeneous small model to the clients, each client can adjust the linear layer dimension of the representation projector to align it with the dimension of the spliced representation. In this way, different clients may hold different representation projectors. When a new model-agnostic client joins in FedMRL, it can adjust its representation projector structure for local model training. Therefore, FedMRL can accommodate FL clients owning local models with diverse structures.

3.2 Multi-Granular Representation Learning

To construct multi-dimensional and multi-granular Matryoshka Representations, we further extract a low-dimension coarse-granularity representation $\tilde{\mathcal{R}}_i^{lc}$ and a high-dimension fine-granularity rep-

representation $\tilde{\mathcal{R}}_i^{hf}$ from the fused representation $\tilde{\mathcal{R}}_i$. They align with the representation dimensions $\{\mathbb{R}^{d_1}, \mathbb{R}^{d_2}\}$ of two feature extractors for matching the parameter dimensions $\{\mathbb{R}^{d_1 \times L}, \mathbb{R}^{d_2 \times L}\}$ of the two prediction headers,

$$\tilde{\mathcal{R}}_i^{lc} = \tilde{\mathcal{R}}_i^{1:d_1}, \tilde{\mathcal{R}}_i^{hf} = \tilde{\mathcal{R}}_i^{1:d_2}. \quad (5)$$

The embedded low-dimension coarse-granularity representation $\tilde{\mathcal{R}}_i^{lc} \in \mathbb{R}^{d_1}$ incorporates coarse generalized and personalized feature information. It is learned by the global homogeneous model header $\mathcal{G}^{hd}(\theta^{hd,t-1})$ (parameter space: $\mathbb{R}^{d_1 \times L}$) with generalized prediction information to produce:

$$\hat{y}_i^{\mathcal{G}} = \mathcal{G}^{hd}(\tilde{\mathcal{R}}_i^{lc}; \theta^{hd,t-1}). \quad (6)$$

The embedded high-dimension fine-granularity representation $\tilde{\mathcal{R}}_i^{hf} \in \mathbb{R}^{d_2}$ carries finer generalized and personalized feature information, which is further processed by the heterogeneous local model header $\mathcal{F}_k^{hd}(\omega_k^{hd,t-1})$ (parameter space: $\mathbb{R}^{d_2 \times L}$) with personalized prediction information to generate:

$$\hat{y}_i^{\mathcal{F}_k} = \mathcal{F}_k^{hd}(\tilde{\mathcal{R}}_i^{hf}; \omega_k^{hd,t-1}). \quad (7)$$

We compute the losses ℓ (e.g., cross-entropy loss [62]) between the two outputs and the label y_i as:

$$\ell_i^{\mathcal{G}} = \ell(\hat{y}_i^{\mathcal{G}}, y_i), \ell_i^{\mathcal{F}_k} = \ell(\hat{y}_i^{\mathcal{F}_k}, y_i). \quad (8)$$

Then, the losses of the two branches are weighted by their importance $m_i^{\mathcal{G}}$ and $m_i^{\mathcal{F}_k}$ and summed as:

$$\ell_i = m_i^{\mathcal{G}} \cdot \ell_i^{\mathcal{G}} + m_i^{\mathcal{F}_k} \cdot \ell_i^{\mathcal{F}_k}. \quad (9)$$

We set $m_i^{\mathcal{G}} = m_i^{\mathcal{F}_k} = 1$ by default to make the two models contribute equally to model performance. The complete loss ℓ_i is used to simultaneously update the homogeneous global small model, the heterogeneous client local model, and the representation projector via gradient descent:

$$\begin{aligned} \theta_k^t &\leftarrow \theta^{t-1} - \eta_\theta \nabla \ell_i, \\ \omega_k^t &\leftarrow \omega_k^{t-1} - \eta_\omega \nabla \ell_i, \\ \varphi_k^t &\leftarrow \varphi_k^{t-1} - \eta_\varphi \nabla \ell_i, \end{aligned} \quad (10)$$

where $\eta_\theta, \eta_\omega, \eta_\varphi$ are the learning rates of the homogeneous global small model, the heterogeneous local model and the representation projector. We set $\eta_\theta = \eta_\omega = \eta_\varphi$ by default to ensure stable model convergence. In this way, the generalized and personalized fused representation is learned from multiple perspectives, thereby improving model learning capability.

4 Convergence Analysis

Based on notations, assumptions and proofs in Appendix B, we analyse the convergence of FedMRL.

Lemma 1 Local Training. *Given Assumptions 1 and 2, the loss of an arbitrary client's local model w in local training round $(t+1)$ is bounded by:*

$$\mathbb{E}[\mathcal{L}_{(t+1)E}] \leq \mathcal{L}_{tE+0} + \left(\frac{L_1 \eta^2}{2} - \eta\right) \sum_{e=0}^E \|\nabla \mathcal{L}_{tE+e}\|_2^2 + \frac{L_1 E \eta^2 \sigma^2}{2}. \quad (11)$$

Lemma 2 Model Aggregation. *Given Assumptions 2 and 3, after local training round $(t+1)$, a client's loss before and after receiving the updated global homogeneous small models is bounded by:*

$$\mathbb{E}[\mathcal{L}_{(t+1)E+0}] \leq \mathbb{E}[\mathcal{L}_{tE+1}] + \eta \delta^2. \quad (12)$$

Theorem 1 One Complete Round of FL. *Given the above lemmas, for any client, after receiving the updated global homogeneous small model, we have:*

$$\mathbb{E}[\mathcal{L}_{(t+1)E+0}] \leq \mathcal{L}_{tE+0} + \left(\frac{L_1 \eta^2}{2} - \eta\right) \sum_{e=0}^E \|\nabla \mathcal{L}_{tE+e}\|_2^2 + \frac{L_1 E \eta^2 \sigma^2}{2} + \eta \delta^2. \quad (13)$$

Theorem 2 Non-convex Convergence Rate of FedMRL. Given Theorem 1, for any client and an arbitrary constant $\epsilon > 0$, the following holds:

$$\frac{1}{T} \sum_{t=0}^{T-1} \sum_{e=0}^{E-1} \|\nabla \mathcal{L}_{tE+e}\|_2^2 \leq \frac{\frac{1}{T} \sum_{t=0}^{T-1} [\mathcal{L}_{tE+0} - \mathbb{E}[\mathcal{L}_{(t+1)E+0}]] + \frac{L_1 E \eta^2 \sigma^2}{2} + \eta \delta^2}{\eta - \frac{L_1 \eta^2}{2}} < \epsilon, \quad (14)$$

$$s.t. \eta < \frac{2(\epsilon - \delta^2)}{L_1(\epsilon + E\sigma^2)}.$$

Therefore, we conclude that any client’s local model can converge at a non-convex rate of $\epsilon \sim \mathcal{O}(1/T)$ in FedMRL if the learning rates of the homogeneous small model, the client local heterogeneous model and the personalized representation projector satisfy the above conditions.

5 Experimental Evaluation

We implement FedMRL on Pytorch, and compare it with seven state-of-the-art MHeteroFL methods. The experiments are carried out over two benchmark supervised image classification datasets on 4 NVIDIA GeForce 3090 GPUs (24GB Memory).³

5.1 Experiment Setup

Datasets. The benchmark datasets adopted are CIFAR-10 and CIFAR-100⁴ [20], which are commonly used in FL image classification tasks for the evaluating existing MHeteroFL algorithms. CIFAR-10 has 60,000 32×32 colour images across 10 classes, with 50,000 for training and 10,000 for testing. CIFAR-100 has 60,000 32×32 colour images across 100 classes, with 50,000 for training and 10,000 for testing. We follow [37] and [34] to construct two types of non-IID datasets. Each client’s non-IID data are further divided into a training set and a testing set with a ratio of 8 : 2.

- **Non-IID (Class):** For CIFAR-10 with 10 classes, we randomly assign 2 classes to each FL client. For CIFAR-100 with 100 classes, we randomly assign 10 classes to each FL client. The fewer classes each client possesses, the higher the non-IIDness.
- **Non-IID (Dirichlet):** To produce more sophisticated non-IID data settings, for each class of CIFAR-10/CIFAR-100, we use a Dirichlet(α) function to adjust the ratio between the number of FL clients and the assigned data. A smaller α indicates more pronounced non-IIDness.

Models. We evaluate MHeteroFL algorithms under model-homogeneous and heterogeneous FL scenarios. FedMRL’s representation projector is a one-layer linear model (parameter space: $\mathbb{R}^{d_2 \times (d_1 + d_2)}$).

- **Model-Homogeneous FL:** All clients train CNN-1 in Table 2 (Appendix C.1). The homogeneous global small models in FML and FedKD are also CNN-1. The extra homogeneous global small model in FedMRL is CNN-1 with a smaller representation dimension d_1 (*i.e.*, the penultimate linear layer dimension) than the CNN-1 model’s representation dimension d_2 , $d_1 \leq d_2$.
- **Model-Heterogeneous FL:** The 5 heterogeneous models {CNN-1, . . . , CNN-5} in Table 2 (Appendix C.1) are evenly distributed among FL clients. The homogeneous global small models in FML and FedKD are the smallest CNN-5 models. The homogeneous global small model in FedMRL is the smallest CNN-5 with a reduced representation dimension d_1 compared with the CNN-5 model representation dimension d_2 , *i.e.*, $d_1 \leq d_2$.

Comparison Baselines. We compare FedMRL with state-of-the-art algorithms belonging to the following three categories of MHeteroFL methods:

- **Standalone.** Each client trains its heterogeneous local model only with its local data.
- **Knowledge Distillation Without Public Data:** FD [19] and FedProto [41].
- **Model Split:** LG-FedAvg [24].

³Codes are available in supplemental materials.

⁴<https://www.cs.toronto.edu/~7Ekriz/cifar.html>

- **Mutual Learning:** FML [38], FedKD [43] and FedAPEN [34].

Evaluation Metrics. We evaluate MHeteroFL algorithms from the following three aspects:

- **Model Accuracy.** We record the test accuracy of each client’s model in each round, and compute the average test accuracy.
- **Communication Cost.** We compute the number of parameters sent between the server and one client in one communication round, and record the required rounds for reaching the target average accuracy. The overall communication cost of one client for target average accuracy is the product between the cost per round and the number of rounds.
- **Computation Overhead.** We compute the computation FLOPs of one client in one communication round, and record the required communication rounds for reaching the target average accuracy. The overall computation overall for one client achieving the target average accuracy is the product between the FLOPs per round and the number of rounds.

Training Strategy. We search optimal FL hyperparameters and unique hyperparameters for all MHeteroFL algorithms. For FL hyperparameters, we test MHeteroFL algorithms with a $\{64, 128, 256, 512\}$ batch size, $\{1, 10\}$ epochs, $T = \{100, 500\}$ communication rounds and an SGD optimizer with a 0.01 learning rate. The unique hyperparameter of FedMRL is the representation dimension d_1 of the homogeneous global small model, we vary $d_1 = \{100, 150, \dots, 500\}$ to obtain the best-performing FedMRL.

5.2 Results and Discussion

We design three FL settings with different numbers of clients (N) and client participation rates (C): ($N = 10, C = 100\%$), ($N = 50, C = 20\%$), ($N = 100, C = 10\%$) for both model-homogeneous and model-heterogeneous FL scenarios.

5.2.1 Average Test Accuracy

Table 1 and Table 3 (Appendix C.2) show that FedMRL consistently outperforms all baselines under both model-heterogeneous or homogeneous settings. It achieves up to a 8.48% improvement in average test accuracy compared with the best baseline under each setting. Furthermore, it achieves up to a 24.94% average test accuracy improvement than the best same-category (*i.e.*, mutual learning-based MHeteroFL) baseline under each setting. These results demonstrate the superiority of FedMRL in model performance owing to its adaptive personalized representation fusion and multi-granularity representation learning capabilities. Figure 3(left six) shows that FedMRL consistently achieves faster convergence speed and higher average test accuracy than the best baseline under each setting.

5.2.2 Individual Client Test Accuracy

Figure 3(right two) shows the difference between the test accuracy achieved by FedMRL vs. the best-performing baseline FedProto (*i.e.*, FedMRL - FedProto) under ($N = 100, C = 10\%$) for each individual client. It can be observed that 87% and 99% of all clients achieve better performance under FedMRL than under FedProto on CIFAR-10 and CIFAR-100, respectively. This demonstrates that FedMRL possesses stronger personalization capability than FedProto owing to its adaptive personalized multi-granularity representation learning design.

5.2.3 Communication Cost

We record the communication rounds and the number of parameters sent per client to achieve 90% and 50% target test average accuracy on CIFAR-10 and CIFAR-100, respectively. Figure 4 (left) shows that FedMRL requires fewer rounds and achieves faster convergence than FedProto. Figure 4 (middle) shows that FedMRL incurs higher communication costs than FedProto as it transmits the full homogeneous small model, while FedProto only transmits each local seen-class average representation between the server and the client. Nevertheless, FedMRL with an optional smaller representation dimension (d_1) of the homogeneous small model still achieves higher communication efficiency than same-category mutual learning-based MHeteroFL baselines (FML, FedKD, FedAPEN) with a larger representation dimension.

Table 1: Average test accuracy (%) in model-heterogeneous FL.

FL Setting	N=10, C=100%		N=50, C=20%		N=100, C=10%	
Method	CIFAR-10	CIFAR-100	CIFAR-10	CIFAR-100	CIFAR-10	CIFAR-100
Standalone	96.53	72.53	95.14	62.71	91.97	53.04
LG-FedAvg [24]	96.30	72.20	94.83	60.95	91.27	45.83
FD [19]	96.21	-	-	-	-	-
FedProto [41]	96.51	72.59	95.48	62.69	92.49	53.67
FML [38]	30.48	16.84	-	21.96	-	15.21
FedKD [43]	80.20	53.23	77.37	44.27	73.21	37.21
FedAPEN [34]	-	-	-	-	-	-
FedMRL	96.63	74.37	95.70	66.04	95.85	62.15
FedMRL-Best B.	0.10	1.78	0.22	3.33	3.36	8.48
FedMRL-Best S.C.B.	16.43	21.14	18.33	21.77	22.64	24.94

“-”: failing to converge. “**█**”: the best MHeteroFL method. “**█** Best B.”: the best baseline. “**█** Best S.C.B.”: the best same-category (mutual learning-based MHeteroFL) baseline. The underscored values denote the largest accuracy improvement of FedMRL across 6 settings.

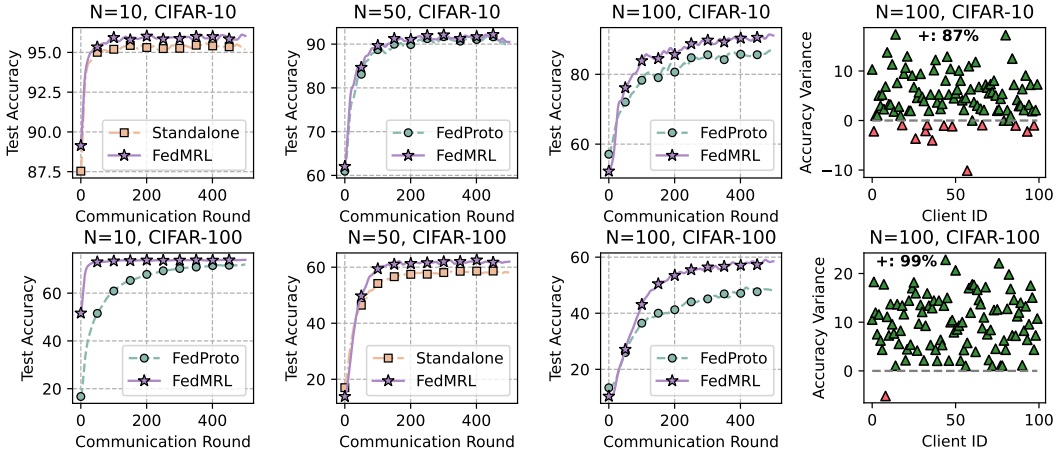


Figure 3: Left six: average test accuracy vs. communication rounds. Right two: individual clients’ test accuracy (%) differences (FedMRL - FedProto).

5.2.4 Computation Overhead

We also calculate the computation FLOPs consumed per client to reach 90% and 50% target average test accuracy on CIFAR-10 and CIFAR-100, respectively. Figure 4(right) shows that FedMRL incurs lower computation costs than FedProto, owing to its faster convergence (*i.e.*, fewer rounds) even with higher computation overhead per round due to the need to train an additional homogeneous small model and a linear representation projector.

5.3 Case Studies

5.3.1 Robustness to Non-IIDness (Class)

We evaluate the robustness of FedMRL to different non-IIDnesses as a result of the number of classes assigned to each client under the ($N = 100, C = 10\%$) setting. The fewer classes assigned to each client, the higher the non-IIDness. For CIFAR-10, we assign $\{2, 4, \dots, 10\}$ classes out of total 10 classes to each client. For CIFAR-100, we assign $\{10, 30, \dots, 100\}$ classes out of total 100 classes to each client. Figure 5(left two) shows that FedMRL consistently achieves higher average test accuracy than the best-performing baseline - FedProto on both datasets, demonstrating its robustness to non-IIDness by class.

5.3.2 Robustness to Non-IIDness (Dirichlet)

We also test the robustness of FedMRL to various non-IIDnesses controlled by α in the Dirichlet function under the ($N = 100, C = 10\%$) setting. A smaller α indicates a higher non-IIDness. For both datasets, we vary α in the range of $\{0.1, \dots, 0.5\}$. Figure 5(right two) shows that FedMRL

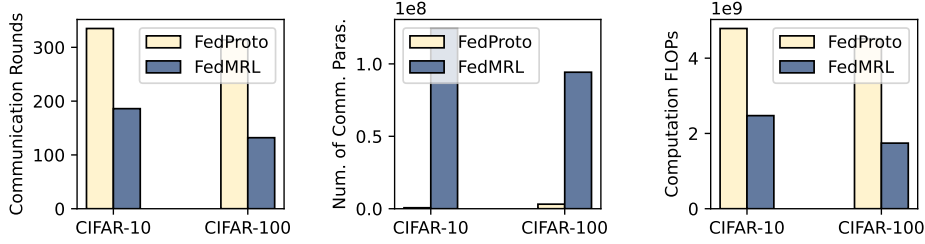


Figure 4: Communication rounds, number of communicated parameters, and computation FLOPs required to reach 90% and 50% average test accuracy targets on CIFAR-10 and CIFAR-100.

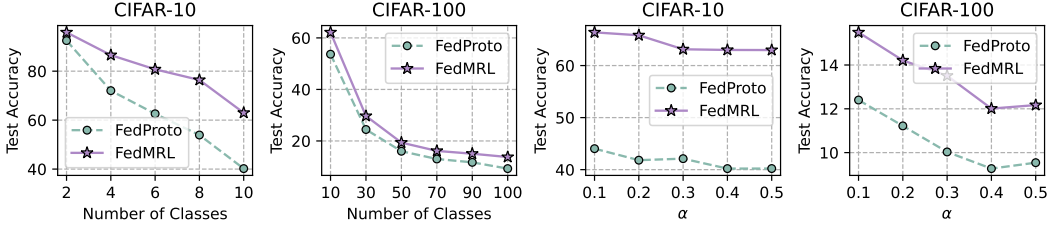


Figure 5: Robustness to non-IIDness (Class & Dirichlet).

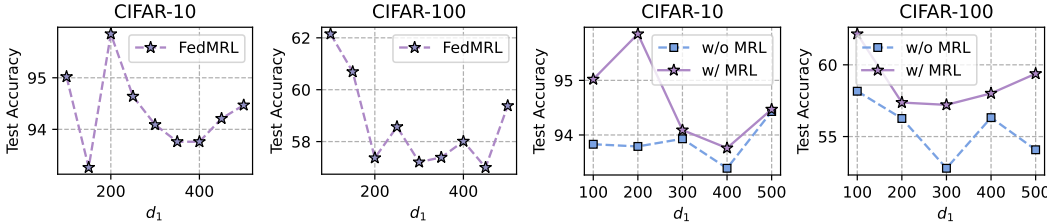


Figure 6: Left two: sensitivity analysis results. Right two: ablation study results.

significantly outperforms FedProto under all non-IIDness settings, validating its robustness to Dirichlet non-IIDness.

5.3.3 Sensitivity Analysis - d_1

FedMRL relies on a hyperparameter d_1 - the representation dimension of the homogeneous small model. To evaluate its sensitivity to d_1 , we test FedMRL with $d_1 = \{100, 150, \dots, 500\}$ under the ($N = 100, C = 10\%$) setting. Figure 6(left two) shows that smaller d_1 values result in higher average test accuracy on both datasets. It is clear that a smaller d_1 also reduces communication and computation overheads, thereby helping FedMRL achieve the best trade-off among model performance, communication efficiency, and computational efficiency.

5.4 Ablation Study

We conduct ablation experiments to validate the usefulness of MRL. For FedMRL with MRL, the global header and the local header learn multi-granularity representations. For FedMRL without MRL, we directly input the representation fused by the representation projector into the client’s local header for loss computation (*i.e.*, we do not extract Matryoshka Representations and remove the global header). Figure 6(right two) shows that FedMRL with MRL consistently outperforms FedMRL without MRL, demonstrating the effectiveness of the design to incorporate MRL into MHeteroFL. Besides, the accuracy gap between them decreases as d_1 rises. This shows that as the global and local headers learn increasingly overlapping representation information, the benefits of MRL are reduced.

6 Conclusions

This paper proposes a novel MHeteroFL approach - FedMRL - to jointly address data, system and model heterogeneity challenges in FL. The key design insight is the addition of a global homogeneous small model shared by FL clients for enhanced knowledge interaction among heterogeneous local

models. Adaptive personalized representation fusion and multi-granularity Matryoshka Representations learning further boosts model learning capability. The client and the server only need to exchange the homogeneous small model, while the clients’ heterogeneous local models and data remain unexposed, thereby enhancing the preservation of both model and data privacy. Theoretical analysis shows that FedMRL is guaranteed to converge over time. Extensive experiments demonstrate that FedMRL significantly outperforms state-of-the-art models regarding test accuracy, while incurring low communication and computation costs.⁵

References

- [1] Jin-Hyun Ahn et al. Wireless federated distillation for distributed edge learning with heterogeneous data. In *Proc. PIMRC*, pages 1–6, Istanbul, Turkey, 2019. IEEE.
- [2] Jin-Hyun Ahn et al. Cooperative learning VIA federated distillation OVER fading channels. In *Proc. ICASSP*, pages 8856–8860, Barcelona, Spain, 2020. IEEE.
- [3] Samiul Alam et al. Fedrolex: Model-heterogeneous federated learning with rolling sub-model extraction. In *Proc. NeurIPS*, virtual, 2022. .
- [4] Sara Babakniya et al. Revisiting sparsity hunting in federated learning: Why does sparsity consensus matter? *Transactions on Machine Learning Research*, 1(1):1, 2023.
- [5] Yun-Hin Chan, Rui Zhou, Running Zhao, Zhihan JIANG, and Edith C. H. Ngai. Internal cross-layer gradients for extending homogeneity to heterogeneity in federated learning. In *Proc. ICLR*, page 1, Vienna, Austria, 2024. OpenReview.net.
- [6] Hongyan Chang et al. Cronus: Robust and heterogeneous collaborative learning with black-box knowledge transfer. In *Proc. NeurIPS Workshop*, virtual, 2021. .
- [7] Jianguai Chen et al. Fedmatch: Federated learning over heterogeneous question answering data. In *Proc. CIKM*, pages 181–190, virtual, 2021. ACM.
- [8] Sijie Cheng et al. Fedgems: Federated learning of larger server models via selective knowledge fusion. *CoRR*, abs/2110.11027, 2021.
- [9] Yae Jee Cho et al. Heterogeneous ensemble knowledge transfer for training large models in federated learning. In *Proc. IJCAI*, pages 2881–2887, virtual, 2022. ijcai.org.
- [10] Liam Collins et al. Exploiting shared representations for personalized federated learning. In *Proc. ICML*, volume 139, pages 2089–2099, virtual, 2021. PMLR.
- [11] Enmao Diao. Heteroffl: Computation and communication efficient federated learning for heterogeneous clients. In *Proc. ICLR*, page 1, Virtual Event, Austria, 2021. OpenReview.net.
- [12] Xuan Gong et al. Federated learning via input-output collaborative distillation. In *Proc. AAI*, pages 22058–22066, Vancouver, Canada, 2024. AAI Press.
- [13] Chaoyang He et al. Group knowledge transfer: Federated learning of large cnns at the edge. In *Proc. NeurIPS*, virtual, 2020. .
- [14] S. Horváth. FjORD: Fair and accurate federated learning under heterogeneous targets with ordered dropout. In *Proc. NIPS*, pages 12876–12889, Virtual, 2021. OpenReview.net.
- [15] Wenke Huang et al. Few-shot model agnostic federated learning. In *Proc. MM*, pages 7309–7316, Lisboa, Portugal, 2022. ACM.
- [16] Wenke Huang et al. Learn from others and be yourself in heterogeneous federated learning. In *Proc. CVPR*, pages 10133–10143, virtual, 2022. IEEE.
- [17] Sohei Itahara et al. Distillation-based semi-supervised federated learning for communication-efficient collaborative training with non-iid private data. *IEEE Trans. Mob. Comput.*, 22(1):191–205, 2023.
- [18] Jaehee Jang et al. Fedclassavg: Local representation learning for personalized federated learning on heterogeneous neural networks. In *Proc. ICPP*, pages 76:1–76:10, virtual, 2022. ACM.

⁵Appendix D discusses FedMRL’s privacy, communication and computation. Appendix E elaborates FedMRL’s border impact and limitations.

- [19] Eunjeong Jeong et al. Communication-efficient on-device machine learning: Federated distillation and augmentation under non-iid private data. In *Proc. NeurIPS Workshop on Machine Learning on the Phone and other Consumer Devices*, virtual, 2018. .
- [20] Alex Krizhevsky et al. *Learning multiple layers of features from tiny images*. Toronto, ON, Canada, , 2009.
- [21] Aditya Kusupati et al. Matryoshka representation learning. In *Proc. NeurIPS*, New Orleans, LA, USA, 2022.
- [22] Daliang Li and Junpu Wang. Fedmd: Heterogenous federated learning via model distillation. In *Proc. NeurIPS Workshop*, virtual, 2019. .
- [23] Qinbin Li et al. Practical one-shot federated learning for cross-silo setting. In *Proc. IJCAI*, pages 1484–1490, virtual, 2021. ijcai.org.
- [24] Paul Pu Liang et al. Think locally, act globally: Federated learning with local and global representations. *arXiv preprint arXiv:2001.01523*, 1(1), 2020.
- [25] Tao Lin et al. Ensemble distillation for robust model fusion in federated learning. In *Proc. NeurIPS*, virtual, 2020. .
- [26] Chang Liu et al. Completely heterogeneous federated learning. *CoRR*, abs/2210.15865, 2022.
- [27] Disha Makhija et al. Architecture agnostic federated learning for neural networks. In *Proc. ICML*, volume 162, pages 14860–14870, virtual, 2022. PMLR.
- [28] Koji Matsuda et al. Fedme: Federated learning via model exchange. In *Proc. SDM*, pages 459–467, Alexandria, VA, USA, 2022. SIAM.
- [29] Brendan McMahan et al. Communication-efficient learning of deep networks from decentralized data. In *Proc. AISTATS*, volume 54, pages 1273–1282, Fort Lauderdale, FL, USA, 2017. PMLR.
- [30] Duy Phuong Nguyen et al. Enhancing heterogeneous federated learning with knowledge extraction and multi-model fusion. In *Proc. SC Workshop*, pages 36–43, Denver, CO, USA, 2023. ACM.
- [31] Jaehoon Oh et al. Fedbabu: Toward enhanced representation for federated image classification. In *Proc. ICLR*, virtual, 2022. OpenReview.net.
- [32] Sejun Park et al. Towards understanding ensemble distillation in federated learning. In *Proc. ICML*, volume 202, pages 27132–27187, Honolulu, Hawaii, USA, 2023. PMLR.
- [33] Krishna Pillutla et al. Federated learning with partial model personalization. In *Proc. ICML*, volume 162, pages 17716–17758, virtual, 2022. PMLR.
- [34] Zhen Qin et al. Fedapen: Personalized cross-silo federated learning with adaptability to statistical heterogeneity. In *Proc. KDD*, pages 1954–1964, Long Beach, CA, USA, 2023. ACM.
- [35] Felix Sattler et al. Fedaux: Leveraging unlabeled auxiliary data in federated learning. *IEEE Trans. Neural Networks Learn. Syst.*, 1(1):1–13, 2021.
- [36] Felix Sattler et al. CFD: communication-efficient federated distillation via soft-label quantization and delta coding. *IEEE Trans. Netw. Sci. Eng.*, 9(4):2025–2038, 2022.
- [37] Aviv Shamsian et al. Personalized federated learning using hypernetworks. In *Proc. ICML*, volume 139, pages 9489–9502, virtual, 2021. PMLR.
- [38] Tao Shen et al. Federated mutual learning. *CoRR*, abs/2006.16765, 2020.
- [39] Xiaorong Shi, Liping Yi, Xiaoguang Liu, and Gang Wang. FFEDCL: fair federated learning with contrastive learning. In *Proc. ICASSP, Rhodes Island, Greece.*, pages 1–5. IEEE, 2023.
- [40] Alysa Ziyang Tan et al. Towards personalized federated learning. *IEEE Trans. Neural Networks Learn. Syst.*, 1(1):1–17, 2022.
- [41] Yue Tan et al. Fedproto: Federated prototype learning across heterogeneous clients. In *Proc. AAAI*, pages 8432–8440, virtual, 2022. AAAI Press.
- [42] Jiaqi Wang et al. Towards personalized federated learning via heterogeneous model reassembly. In *Proc. NeurIPS*, page 13, New Orleans, Louisiana, USA, 2023. OpenReview.net.

- [43] Chuhan Wu et al. Communication-efficient federated learning via knowledge distillation. *Nature Communications*, 13(1):2032, 2022.
- [44] Liping Yi, Xiaorong Shi, Nan Wang, Gang Wang, Xiaoguang Liu, Zhuan Shi, and Han Yu. pfdkt: Personalized federated learning with dual knowledge transfer. *Knowledge-Based Systems*, 292:111633, 2024.
- [45] Liping Yi, Xiaorong Shi, Nan Wang, Ziyue Xu, Gang Wang, and Xiaoguang Liu. pfdlhrs: Personalized federated learning via local hypernetworks. In *Proc. ICANN*, volume 1, page 516–528. Springer, 2023.
- [46] Liping Yi, Xiaorong Shi, Nan Wang, Jinsong Zhang, Gang Wang, and Xiaoguang Liu. Fedpe: Adaptive model pruning-expanding for federated learning on mobile devices. *IEEE Transactions on Mobile Computing*, pages 1–18, 2024.
- [47] Liping Yi, Xiaorong Shi, Wenrui Wang, Gang Wang, and Xiaoguang Liu. Fedrra: Reputation-aware robust federated learning against poisoning attacks. In *Proc. IJCNN*, pages 1–8. IEEE, 2023.
- [48] Liping Yi, Gang Wang, and Xiaoguang Liu. QSFL: A two-level uplink communication optimization framework for federated learning. In *Proc. ICML*, volume 162, pages 25501–25513. PMLR, 2022.
- [49] Liping Yi, Gang Wang, Xiaoguang Liu, Zhuan Shi, and Han Yu. Fedgh: Heterogeneous federated learning with generalized global header. In *Proceedings of the 31st ACM International Conference on Multimedia (ACM MM’23)*, page 11, Canada, 2023. ACM.
- [50] Liping Yi, Han Yu, Chao Ren, Heng Zhang, Gang Wang, Xiaoguang Liu, and Xiaoxiao Li. pfdafm: Adaptive feature mixture for batch-level personalization in heterogeneous federated learning. *CoRR*, abs/2404.17847, 2024.
- [51] Liping Yi, Han Yu, Chao Ren, Heng Zhang, Gang Wang, Xiaoguang Liu, and Xiaoxiao Li. pfdmoe: Data-level personalization with mixture of experts for model-heterogeneous personalized federated learning. *CoRR*, abs/2402.01350, 2024.
- [52] Liping Yi, Han Yu, Zhuan Shi, Gang Wang, Xiaoguang Liu, Lizhen Cui, and Xiaoxiao Li. FedSSA: Semantic Similarity-based Aggregation for Efficient Model-Heterogeneous Personalized Federated Learning. In *IJCAI*, 2024.
- [53] Liping Yi, Han Yu, Gang Wang, and Xiaoguang Liu. Fedlora: Model-heterogeneous personalized federated learning with lora tuning. *CoRR*, abs/2310.13283, 2023.
- [54] Liping Yi, Han Yu, Gang Wang, and Xiaoguang Liu. pfdes: Model heterogeneous personalized federated learning with feature extractor sharing. *CoRR*, abs/2311.06879, 2023.
- [55] Liping Yi, Jinsong Zhang, Rui Zhang, Jiaqi Shi, Gang Wang, and Xiaoguang Liu. Su-net: An efficient encoder-decoder model of federated learning for brain tumor segmentation. In *Proc. ICANN*, volume 12396, pages 761–773. Springer, 2020.
- [56] Fuxun Yu et al. Fed2: Feature-aligned federated learning. In *Proc. KDD*, pages 2066–2074, virtual, 2021. ACM.
- [57] Sixing Yu et al. Resource-aware federated learning using knowledge extraction and multi-model fusion. *CoRR*, abs/2208.07978, 2022.
- [58] Jianqing Zhang, Yang Liu, Yang Hua, and Jian Cao. Fedtgp: Trainable global prototypes with adaptive-margin-enhanced contrastive learning for data and model heterogeneity in federated learning. In *Proc. AAAI*, pages 16768–16776, Vancouver, Canada, 2024. AAAI Press.
- [59] Jie Zhang et al. Parameterized knowledge transfer for personalized federated learning. In *Proc. NeurIPS*, pages 10092–10104, virtual, 2021. OpenReview.net.
- [60] Jie Zhang et al. Towards data-independent knowledge transfer in model-heterogeneous federated learning. *IEEE Trans. Computers*, 72(10):2888–2901, 2023.
- [61] Lan Zhang et al. Fedzkt: Zero-shot knowledge transfer towards resource-constrained federated learning with heterogeneous on-device models. In *Proc. ICDCS*, pages 928–938, virtual, 2022. IEEE.
- [62] Zhilu Zhang and Mert R. Sabuncu. Generalized cross entropy loss for training deep neural networks with noisy labels. In *Proc. NeurIPS*, pages 8792–8802, Montréal, Canada, 2018. Curran Associates Inc.
- [63] Zhuangdi Zhu et al. Data-free knowledge distillation for heterogeneous federated learning. In *Proc. ICML*, volume 139, pages 12878–12889, virtual, 2021. PMLR.
- [64] Zhuangdi Zhu et al. Resilient and communication efficient learning for heterogeneous federated systems. In *Proc. ICML*, volume 162, pages 27504–27526, virtual, 2022. PMLR.

A Pseudo codes of FedMRL

Algorithm 1: FedMRL

Input: N , total number of clients; K , number of selected clients in one round; T , total number of rounds; η_ω , learning rate of client local heterogeneous models; η_θ , learning rate of homogeneous small model; η_φ , learning rate of the representation projector.

Output: client whole models removing the global header

$$[\mathcal{G}(\theta^{ex,T-1}) \circ \mathcal{F}_0(\omega_0^{T-1}) | \mathcal{P}_0(\varphi_0^{T-1}), \dots, \mathcal{G}(\theta^{ex,T-1}) \circ \mathcal{F}_{N-1}(\omega_{N-1}^{T-1}) | \mathcal{P}_{N-1}(\varphi_{N-1}^{T-1})].$$

Randomly initialize the global homogeneous small model $\mathcal{G}(\theta^0)$, client local heterogeneous models $[\mathcal{F}_0(\omega_0^0), \dots, \mathcal{F}_{N-1}(\omega_{N-1}^0)]$ and local heterogeneous representation projectors

$$[\mathcal{P}_0(\varphi_0^0), \dots, \mathcal{P}_{N-1}(\varphi_{N-1}^0)].$$

for each round $t=1, \dots, T-1$ do

// Server Side:

$S^t \leftarrow$ Randomly sample K clients from N clients;

 Broadcast the global homogeneous small model θ^{t-1} to sampled K clients;

$\theta_k^t \leftarrow$ **ClientUpdate**(θ^{t-1});

 /* Aggregate Local Homogeneous Small Models */

$$\theta^t = \sum_{k=0}^{K-1} \frac{n_k}{n} \theta_k^t.$$

// ClientUpdate:

 Receive the global homogeneous small model θ^{t-1} from the server;

for $k \in S^t$ do

 /* Local Training with MRL */

for $(\mathbf{x}_i, y_i) \in D_k$ do

$$\mathcal{R}_i^{\mathcal{G}} = \mathcal{G}^{ex}(\mathbf{x}_i; \theta^{ex,t-1}), \mathcal{R}_i^{\mathcal{F}_k} = \mathcal{F}_k^{ex}(\mathbf{x}_i; \omega_k^{ex,t-1});$$

$$\mathcal{R}_i = \mathcal{R}_i^{\mathcal{G}} \circ \mathcal{R}_i^{\mathcal{F}_k};$$

$$\tilde{\mathcal{R}}_i = \mathcal{P}_k(\mathcal{R}_i; \varphi_k^{t-1});$$

$$\tilde{\mathcal{R}}_i^{lc} = \tilde{\mathcal{R}}_i^{1:d_1}, \tilde{\mathcal{R}}_i^{hf} = \tilde{\mathcal{R}}_i^{1:d_2};$$

$$\hat{y}_i^{\mathcal{G}} = \mathcal{G}^{hd}(\tilde{\mathcal{R}}_i^{lc}; \theta^{hd,t-1}); \hat{y}_i^{\mathcal{F}_k} = \mathcal{F}_k^{hd}(\omega_k^{hd,t-1});$$

$$\ell_i^{\mathcal{G}} = \ell(\hat{y}_i^{\mathcal{G}}, y_i); \ell_i^{\mathcal{F}_k} = \ell(\hat{y}_i^{\mathcal{F}_k}, y_i);$$

$$\ell_i = m_i^{\mathcal{G}} \cdot \ell_i^{\mathcal{G}} + m_i^{\mathcal{F}_k} \cdot \ell_i^{\mathcal{F}_k};$$

$$\theta_k^t \leftarrow \theta^{t-1} - \eta_\theta \nabla \ell_i;$$

$$\omega_k^t \leftarrow \omega_k^{t-1} - \eta_\omega \nabla \ell_i;$$

$$\varphi_k^t \leftarrow \varphi_k^{t-1} - \eta_\varphi \nabla \ell_i;$$

end

 Upload updated local homogeneous small model θ_k^t to the server.

end

end

B Theoretical Proofs

We first define the following additional notations. $t \in \{0, \dots, T-1\}$ denotes the t -th round. $e \in \{0, 1, \dots, E\}$ denotes the e -th iteration of local training. $tE+0$ indicates that clients receive the global homogeneous small model $\mathcal{G}(\theta^t)$ from the server before the $(t+1)$ -th round's local training. $tE+e$ denotes the e -th iteration of the $(t+1)$ -th round's local training. $tE+E$ marks the ending of the $(t+1)$ -th round's local training. After that, clients upload their updated local homogeneous small models to the server for aggregation. $\mathcal{W}_k(w_k)$ denotes the whole model trained on client k , including the global homogeneous small model $\mathcal{G}(\theta)$, the client k 's local heterogeneous model $\mathcal{F}_k(w_k)$, and the personalized representation projector $\mathcal{P}_k(\varphi_k)$. η is the learning rate of the whole model trained on client k , including $\{\eta_\theta, \eta_\omega, \eta_\varphi\}$.

Assumption 1 Lipschitz Smoothness. *The gradients of client k 's whole local model w_k are L_1 -Lipschitz smooth [41],*

$$\begin{aligned} \|\nabla \mathcal{L}_k^{t_1}(w_k^{t_1}; \mathbf{x}, y) - \nabla \mathcal{L}_k^{t_2}(w_k^{t_2}; \mathbf{x}, y)\| &\leq L_1 \|w_k^{t_1} - w_k^{t_2}\|, \\ \forall t_1, t_2 > 0, k \in \{0, 1, \dots, N-1\}, (\mathbf{x}, y) \in D_k. \end{aligned} \quad (15)$$

The above formulation can be re-expressed as:

$$\mathcal{L}_k^{t_1} - \mathcal{L}_k^{t_2} \leq \langle \nabla \mathcal{L}_k^{t_2}, (w_k^{t_1} - w_k^{t_2}) \rangle + \frac{L_1}{2} \|w_k^{t_1} - w_k^{t_2}\|_2^2. \quad (16)$$

Assumption 2 Unbiased Gradient and Bounded Variance. Client k 's random gradient $g_{w,k}^t = \nabla \mathcal{L}_k^t(w_k^t; \mathcal{B}_k^t)$ (\mathcal{B} is a batch of local data) is unbiased,

$$\mathbb{E}_{\mathcal{B}_k^t \subseteq D_k} [g_{w,k}^t] = \nabla \mathcal{L}_k^t(w_k^t), \quad (17)$$

and the variance of random gradient $g_{w,k}^t$ is bounded by:

$$\mathbb{E}_{\mathcal{B}_k^t \subseteq D_k} [\|\nabla \mathcal{L}_k^t(w_k^t; \mathcal{B}_k^t) - \nabla \mathcal{L}_k^t(w_k^t)\|_2^2] \leq \sigma^2. \quad (18)$$

Assumption 3 Bounded Parameter Variation. The parameter variations of the homogeneous small model θ_k^t and θ^t before and after aggregation at the FL server are bounded by:

$$\|\theta^t - \theta_k^t\|_2^2 \leq \delta^2. \quad (19)$$

B.1 Proof of Lemma 1

Proof 1 An arbitrary client k 's local whole model w can be updated by $w_{t+1} = w_t - \eta g_{w,t}$ in the $(t+1)$ -th round, and following Assumption 1, we can obtain

$$\begin{aligned} \mathcal{L}_{tE+1} &\leq \mathcal{L}_{tE+0} + \langle \nabla \mathcal{L}_{tE+0}, (w_{tE+1} - w_{tE+0}) \rangle + \frac{L_1}{2} \|w_{tE+1} - w_{tE+0}\|_2^2 \\ &= \mathcal{L}_{tE+0} - \eta \langle \nabla \mathcal{L}_{tE+0}, g_{w,tE+0} \rangle + \frac{L_1 \eta^2}{2} \|g_{w,tE+0}\|_2^2. \end{aligned} \quad (20)$$

Taking the expectation of both sides of the inequality concerning the random variable ξ_{tE+0} ,

$$\begin{aligned} \mathbb{E}[\mathcal{L}_{tE+1}] &\leq \mathcal{L}_{tE+0} - \eta \mathbb{E}[\langle \nabla \mathcal{L}_{tE+0}, g_{w,tE+0} \rangle] + \frac{L_1 \eta^2}{2} \mathbb{E}[\|g_{w,tE+0}\|_2^2] \\ &\stackrel{(a)}{=} \mathcal{L}_{tE+0} - \eta \|\nabla \mathcal{L}_{tE+0}\|_2^2 + \frac{L_1 \eta^2}{2} \mathbb{E}[\|g_{w,tE+0}\|_2^2] \\ &\stackrel{(b)}{\leq} \mathcal{L}_{tE+0} - \eta \|\nabla \mathcal{L}_{tE+0}\|_2^2 + \frac{L_1 \eta^2}{2} (\mathbb{E}[\|g_{w,tE+0}\|_2^2] + \text{Var}(g_{w,tE+0})) \\ &\stackrel{(c)}{=} \mathcal{L}_{tE+0} - \eta \|\nabla \mathcal{L}_{tE+0}\|_2^2 + \frac{L_1 \eta^2}{2} (\|\nabla \mathcal{L}_{tE+0}\|_2^2 + \text{Var}(g_{w,tE+0})) \\ &\stackrel{(d)}{\leq} \mathcal{L}_{tE+0} - \eta \|\nabla \mathcal{L}_{tE+0}\|_2^2 + \frac{L_1 \eta^2}{2} (\|\nabla \mathcal{L}_{tE+0}\|_2^2 + \sigma^2) \\ &= \mathcal{L}_{tE+0} + \left(\frac{L_1 \eta^2}{2} - \eta\right) \|\nabla \mathcal{L}_{tE+0}\|_2^2 + \frac{L_1 \eta^2 \sigma^2}{2}. \end{aligned} \quad (21)$$

(a), (c), (d) follow Assumption 2 and (b) follows $\text{Var}(x) = \mathbb{E}[x^2] - (\mathbb{E}[x])^2$.

Taking the expectation of both sides of the inequality for the model w over E iterations, we obtain

$$\mathbb{E}[\mathcal{L}_{tE+1}] \leq \mathcal{L}_{tE+0} + \left(\frac{L_1 \eta^2}{2} - \eta\right) \sum_{e=1}^E \|\nabla \mathcal{L}_{tE+e}\|_2^2 + \frac{L_1 E \eta^2 \sigma^2}{2}. \quad (22)$$

B.2 Proof of Lemma 2

Proof 2

$$\begin{aligned} \mathcal{L}_{(t+1)E+0} &= \mathcal{L}_{(t+1)E} + \mathcal{L}_{(t+1)E+0} - \mathcal{L}_{(t+1)E} \\ &\stackrel{(a)}{\approx} \mathcal{L}_{(t+1)E} + \eta \|\theta_{(t+1)E+0} - \theta_{(t+1)E}\|_2^2 \\ &\stackrel{(b)}{\leq} \mathcal{L}_{(t+1)E} + \eta \delta^2. \end{aligned} \quad (23)$$

(a): we can use the gradient of parameter variations to approximate the loss variations, i.e., $\Delta\mathcal{L} \approx \eta \cdot \|\Delta\theta\|_2^2$. (b) follows Assumption 3.

Taking the expectation of both sides of the inequality to the random variable ξ , we obtain

$$\mathbb{E}[\mathcal{L}_{(t+1)E+0}] \leq \mathbb{E}[\mathcal{L}_{tE+1}] + \eta\delta^2. \quad (24)$$

B.3 Proof of Theorem 1

Proof 3 Substituting Lemma 1 into the right side of Lemma 2's inequality, we obtain

$$\mathbb{E}[\mathcal{L}_{(t+1)E+0}] \leq \mathcal{L}_{tE+0} + \left(\frac{L_1\eta^2}{2} - \eta\right) \sum_{e=0}^E \|\nabla\mathcal{L}_{tE+e}\|_2^2 + \frac{L_1E\eta^2\sigma^2}{2} + \eta\delta^2. \quad (25)$$

B.4 Proof of Theorem 2

Proof 4 Interchanging the left and right sides of Eq. (25), we obtain

$$\sum_{e=0}^E \|\nabla\mathcal{L}_{tE+e}\|_2^2 \leq \frac{\mathcal{L}_{tE+0} - \mathbb{E}[\mathcal{L}_{(t+1)E+0}] + \frac{L_1E\eta^2\sigma^2}{2} + \eta\delta^2}{\eta - \frac{L_1\eta^2}{2}}. \quad (26)$$

Taking the expectation of both sides of the inequality over rounds $t = [0, T-1]$ to w , we obtain

$$\frac{1}{T} \sum_{t=0}^{T-1} \sum_{e=0}^{E-1} \|\nabla\mathcal{L}_{tE+e}\|_2^2 \leq \frac{\frac{1}{T} \sum_{t=0}^{T-1} [\mathcal{L}_{tE+0} - \mathbb{E}[\mathcal{L}_{(t+1)E+0}]] + \frac{L_1E\eta^2\sigma^2}{2} + \eta\delta^2}{\eta - \frac{L_1\eta^2}{2}}. \quad (27)$$

Let $\Delta = \mathcal{L}_{t=0} - \mathcal{L}^* > 0$, then $\sum_{t=0}^{T-1} [\mathcal{L}_{tE+0} - \mathbb{E}[\mathcal{L}_{(t+1)E+0}]] \leq \Delta$, we can get

$$\frac{1}{T} \sum_{t=0}^{T-1} \sum_{e=0}^{E-1} \|\nabla\mathcal{L}_{tE+e}\|_2^2 \leq \frac{\frac{\Delta}{T} + \frac{L_1E\eta^2\sigma^2}{2} + \eta\delta^2}{\eta - \frac{L_1\eta^2}{2}}. \quad (28)$$

If the above equation converges to a constant ϵ , i.e.,

$$\frac{\frac{\Delta}{T} + \frac{L_1E\eta^2\sigma^2}{2} + \eta\delta^2}{\eta - \frac{L_1\eta^2}{2}} < \epsilon, \quad (29)$$

then

$$T > \frac{\Delta}{\epsilon(\eta - \frac{L_1\eta^2}{2}) - \frac{L_1E\eta^2\sigma^2}{2} - \eta\delta^2}. \quad (30)$$

Since $T > 0$, $\Delta > 0$, we can get

$$\epsilon(\eta - \frac{L_1\eta^2}{2}) - \frac{L_1E\eta^2\sigma^2}{2} - \eta\delta^2 > 0. \quad (31)$$

Solving the above inequality yields

$$\eta < \frac{2(\epsilon - \delta^2)}{L_1(\epsilon + E\sigma^2)}. \quad (32)$$

Since ϵ , L_1 , σ^2 , δ^2 are all constants greater than 0, η has solutions. Therefore, when the learning rate $\eta = \{\eta_\theta, \eta_\omega, \eta_\varphi\}$ satisfies the above condition, any client's local whole model can converge. Since all terms on the right side of Eq. (28) except for $1/T$ are constants, hence FedMRL's non-convex convergence rate is $\epsilon \sim \mathcal{O}(1/T)$.

C More Experimental Details

Here, we provide more experimental details of used model structures, more experimental results of model-homogeneous FL scenarios, and also the experimental evidence of inference model selection.

C.1 Model Structures

Table 2 shows the structures of models used in experiments.

Table 2: Structures of 5 heterogeneous CNN models.

Layer Name	CNN-1	CNN-2	CNN-3	CNN-4	CNN-5
Conv1	5×5, 16	5×5, 16	5×5, 16	5×5, 16	5×5, 16
Maxpool1	2×2	2×2	2×2	2×2	2×2
Conv2	5×5, 32	5×5, 16	5×5, 32	5×5, 32	5×5, 32
Maxpool2	2×2	2×2	2×2	2×2	2×2
FC1	2000	2000	1000	800	500
FC2	500	500	500	500	500
FC3	10/100	10/100	10/100	10/100	10/100
model size	10.00 MB	6.92 MB	5.04 MB	3.81 MB	2.55 MB

Note: 5 × 5 denotes kernel size. 16 or 32 are filters in convolutional layers.

C.2 Homogeneous FL Results

Table 3 presents the results of FedMRL and baselines in model-homogeneous FL scenarios.

Table 3: Average test accuracy (%) in model-homogeneous FL.

FL Setting	N=10, C=100%		N=50, C=20%		N=100, C=10%	
	CIFAR-10	CIFAR-100	CIFAR-10	CIFAR-100	CIFAR-10	CIFAR-100
Standalone	96.35	74.32	95.25	62.38	92.58	54.93
LG-FedAvg [24]	96.47	73.43	94.20	61.77	90.25	46.64
FD [19]	96.30	-	-	-	-	-
FedProto [41]	95.83	72.79	95.10	62.55	91.19	54.01
FML [38]	94.83	70.02	93.18	57.56	87.93	46.20
FedKD [43]	94.77	70.04	92.93	57.56	90.23	50.99
FedAPEN [34]	95.38	71.48	93.31	57.62	87.97	46.85
FedMRL	96.71	74.52	95.76	66.46	95.52	60.64
FedMRL-Best B.	0.24	0.20	0.51	3.91	2.94	5.71
FedMRL-Best S.C.B.	1.33	3.04	2.45	8.84	5.29	9.65

“-”: failing to converge. “**█**”: the best MHeteroFL method. “**█** Best B.”: the best baseline. “**█** Best S.C.B.”: the best same-category (mutual learning-based MHeteroFL) baseline. The underscored values denote the largest accuracy improvement of FedMRL across 6 settings.

C.3 Inference Model Comparison

There are 4 alternative models for model inference in FedMRL: (1) mix-small (the combination of the homogeneous small model, the client heterogeneous model’s feature extractor, and the representation projector, *i.e.*, removing the local header), (2) mix-large (the combination of the homogeneous small model’s feature extractor, the client heterogeneous model, and the representation projector, *i.e.*, removing the global header), (3) single-small (the homogeneous small model), (4) single-large (the client heterogeneous model). We compare their model performances under ($N = 100, C = 10\%$) settings. Figure 7 presents that mix-small has a similar accuracy to mix-large which is used as the default inference model, and they significantly outperform the single homogeneous small model and the single heterogeneous client model. Therefore, users can choose mix-small or mix-large for model inference based on their inference costs in practical applications.

D Discussion

We discuss how FedMRL tackles heterogeneity and its privacy, communication and computation.

Tackling Heterogeneity. FedMRL allows each client to tailor its heterogeneous local model according to its system resources, which addresses system and model heterogeneity. Each client achieves multi-granularity representation learning adapting to local non-IID data distribution through a personalized heterogeneous representation projector, alleviating data heterogeneity.

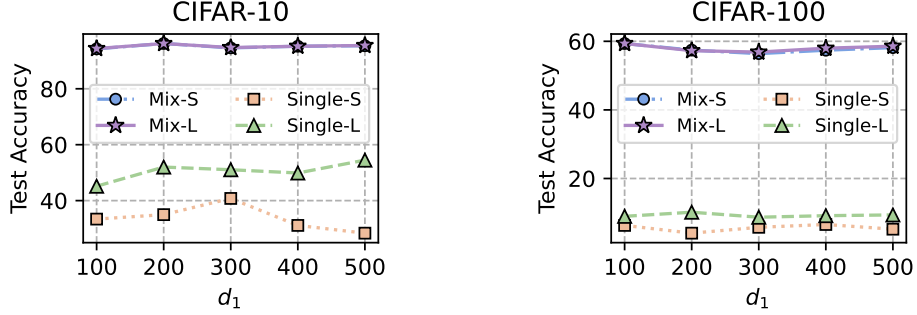


Figure 7: Accuracy of four optional inference models: mix-small (the whole model without the local header), mix-large (the whole model without the global header), single-small (the homogeneous small model), single-large (the client heterogeneous model).

Privacy. The server and clients communicate the homogeneous small models while the heterogeneous local model is always stored in the client. Besides, representation splicing enables the structures of the homogeneous global model and the heterogeneous local model to be not related. Therefore, the parameters and structure privacy of the heterogeneous client model is protected strongly. Meanwhile, the local data are always stored in clients for local training, so local data privacy is also protected.

Communication Cost. The server and clients transmit homogeneous small models with fewer parameters than the client’s heterogeneous local model, consuming significantly lower communication costs in one communication round compared with transmitting complete local models like FedAvg.

Computational Overhead. Except for training the client’s heterogeneous local model, each client also trains the homogeneous global small model and a lightweight representation projector which have far fewer parameters than the heterogeneous local model. The computational overhead in one training round is slightly increased. Since we design personalized Matryoshka Representations learning adapting to local data distribution from multiple perspectives, the model learning capability is improved, accelerating model convergence and consuming fewer training rounds. Therefore, the total computational cost may also be reduced.

E Broader Impacts and Limitations

Broader Impacts. FedMRL improves model performance, communication and computational efficiency for heterogeneous federated learning while effectively protecting the privacy of the client heterogeneous local model and non-IID data. It can be applied in various practical FL applications.

Limitations. The multi-granularity embedded representations within Matryoshka Representations are processed by the global small model’s header and the local client model’s header, respectively. This increases the storage cost, communication costs and training overhead for the global header even though it only involves one linear layer. In future work, we will follow the more effective Matryoshka Representation learning method (MRL-E) [21], removing the global header and only using the local model header to process multi-granularity Matryoshka Representations simultaneously, to enable a better trade-off among model performance and costs of storage, communication and computation.